



This is a repository copy of *Bi-level optimization of sizing and control strategy of hybrid energy storage system in urban rail transit considering substation operation stability*.

White Rose Research Online URL for this paper:

<https://eprints.whiterose.ac.uk/214458/>

Version: Accepted Version

Article:

Dong, H., Tian, Z. orcid.org/0000-0001-7295-3327, Spencer, J.W. et al. (2 more authors) (2024) Bi-level optimization of sizing and control strategy of hybrid energy storage system in urban rail transit considering substation operation stability. *IEEE Transactions on Transportation Electrification*, 10 (4). pp. 10102-10114. ISSN 2332-7782

<https://doi.org/10.1109/tte.2024.3385821>

© 2024 The Authors. Except as otherwise noted, this author-accepted version of a journal article published in *IEEE Transactions on Transportation Electrification* is made available via the University of Sheffield Research Publications and Copyright Policy under the terms of the Creative Commons Attribution 4.0 International License (CC-BY 4.0), which permits unrestricted use, distribution and reproduction in any medium, provided the original work is properly cited. To view a copy of this licence, visit <http://creativecommons.org/licenses/by/4.0/>

Reuse

This article is distributed under the terms of the Creative Commons Attribution (CC BY) licence. This licence allows you to distribute, remix, tweak, and build upon the work, even commercially, as long as you credit the authors for the original work. More information and the full terms of the licence here: <https://creativecommons.org/licenses/>

Takedown

If you consider content in White Rose Research Online to be in breach of UK law, please notify us by emailing eprints@whiterose.ac.uk including the URL of the record and the reason for the withdrawal request.



eprints@whiterose.ac.uk
<https://eprints.whiterose.ac.uk/>

Bi-level Optimization of Sizing and Control Strategy of Hybrid Energy Storage System in Urban Rail Transit Considering Substation Operation Stability

Hongzhi Dong, *Student Member, IEEE*, Zhongbei Tian *Member, IEEE*, Joseph W. Spencer, David Fletcher, Siavash Hajiabady

Abstract—The hybrid energy storage system (HESS) which consists of battery and ultracapacitor can efficiently reduce the substation energy cost from grid and achieve the peak shaving function, due to its characteristics of high-power density and high-energy density. The sizing of HESS affects the operation cost of whole system. Besides, operation stability (like substation peak power and voltage fluctuations) is rarely considered in urban rail transit (URT) when sizing optimization of HESS is considered. Thus, this research proposes a sizing and control strategy optimization of HESS in URT. First, the mathematic model of URT with HESS is established, which is used to simulate URT and HESS operation state by power flow analysis method. Then, based on the proposed HESS control principle, a bi-level optimization of HESS in URT is proposed. The master level aims to optimize the rated capacity and power of HESS, reducing total operational cost. Then, the HESS control strategy is optimized at slave level, reducing substation peak power and voltage fluctuations of URT. The case study is conducted based on the data of Merseyrail line in Liverpool. A comparison is also conducted, which shows that the proposed method can reduce daily operation cost by 12.68% of the substation, while the grid energy cost is decreased by 57.26%.

Index Terms—Urban railway transit, hybrid energy storage system, bi-level optimization

NOMENCLATURE

Variables

v	Train velocity [m/s]
s	Train position [m]
m_{eq}	Train equivalent mass [t]
m_0	Empty train mass [t]
m_l	Load mass [t]
λ	Dimensionless rotating mass factor
F_{veh}	Train traction force [N]
F_r	Train resistance force [N]

k_0	Resistance coefficients [N]
k_1	Resistance coefficients [N/(m/s)]
k_2	Resistance coefficients [N/(m/s) ²]
P_{me}	Train mechanical power [W]
P_{el}	Train electrical power [W]
U_l	Catenary voltage [V]
η	Traction chain conversion efficiency
U_{sub}	Substation voltage [V]
U_{OC}	Substation no-load voltage [V]
I_{sub}	Substation current [A]
R_{sub}	Substation resistance [Ω]
I_B	Current of battery [A]
R_B	Battery resistance [Ω]
U_B	Voltage source of battery [V]
U_{Bat}	Voltage of battery [V]
U_{BESS}	Voltage of BESS [V]
I_{BESS}	Current of BESS [A]
SOC_B	State of charge of BESS
$SOC_{B_initial}$	Initial SOC of BESS
η_B	Efficiency of BESS
T_{B_life}	Battery lifetime [year]
$\alpha_1, \alpha_2, \alpha_3, \alpha_4$	Fixed parameter for lead–acid batteries
DOD	Depth of discharge [%]
k_{cycle}	Full or half cycle coefficient
I	Total battery cycles
U_C	Capacitor voltage [V]
C_U	Capacitance [F]
I_C	Capacitor current [A]
U_{UC}	Ultracapacitor voltage [V]
R_C	Ultracapacitor resistance [Ω]
I_{UC}	Ultracapacitor current [A]
U_{UCESS}	UCESS voltage [V]
I_{UCESS}	UCESS current [A]
SOC_{UC}	State of charge of UCESS
U_{thre_d}	HESS discharge threshold voltage [V]
U_{thre_c}	HESS charge threshold voltage [V]
P_{dis_req}	Required traction power from URT [W]

This research is supported by the EPSRC (Connected and Coordinated Train Operation and Traction Power Supply Systems (COOPS), grant reference EP/Y003136/1). The corresponding author is Zhongbei Tian.

Hongzhi Dong is with the Department of Electrical Engineering and Electronics, University of Liverpool, Liverpool, U.K. (e-mail: Hongzhi.dong@liverpool.ac.uk).

Zhongbei Tian is with the School of Engineering, University of Birmingham, Birmingham, U.K. (e-mail: z.tian@bham.ac.uk).

Joseph W. Spencer is with the Department of Electrical Engineering and Electronics, University of Liverpool, Liverpool, U.K. (e-mail: Joe@liverpool.ac.uk).

David Fletcher is with the Department of Mechanical Engineering, University of Sheffield, Sheffield, U.K. (e-mail: D.I.Fletcher@Sheffield.ac.uk).

Siavash Hajiabady is currently a Principal Traction Engineer at ETAP Automation Ltd U.K. (email: Siavash.Hajiabady@etap.com)

P_{ch}	Total RBE injected to the HESS [W]
P_{HESS_ch}	Charge power of HESS [W]
P_{UC_ch}, P_{B_ch}	Charge power of UCESS and BESS [W]
SOC_{UC_in}, SOC_{B_in}	Initial SOC of UCESS and BESS
$SOC_{UC_end}, SOC_{B_end}$	Final SOC of UCESS and BESS
T_{UC_ch} and T_{B_ch}	Total charge time of UCESS and BESS [s]
t	System operation time t [s]
C_{HESS}	Comprehensive cost of HESS [GBP/day]
C_{cap}	Capital cost of HESS [GBP/day]
C_{rep}	Replacement cost of battery [GBP/day]
COM	O&M cost [GBP/day]
C_{sal}	Salvage value of battery [GBP/day]
T_{op}	Operation days of HESS [day]
k_{CRF}	Capital recovery factor
T_{proj}	Project service period [year]
r_0	Annual discount rate
P_{UC_rated}	Rated power of UCESS [W]
E_{UC_rated}	Rated capacity of UCESS [kWh]
P_{B_rated}	Rated power of BESS [W]
E_{B_rated}	Rated capacity of BESS [kWh]
ρ_{B_p}	Price of BESS rated power [GBP/kW]
ρ_{UC_p}	Price of UCESS rated power [GBP/kW]
ρ_{B_E}	Price of BESS rated capacity [[GBP/kWh]]
ρ_{UC_E}	Price of UCESS rated capacity [[GBP/kWh]]
N_{rep}	Total number of replacements of BESS
ρ_{BE_rep}	Replacement cost of BESS [GBP/MWh]
COM_f	Fixed O&M annual cost [GBP/day]
COM_v	Variable O&M cost [GBP/day]
$\rho_{B_OM_f}$	BESS fixed O&M price [GBP/kW/year]
$\rho_{UC_OM_f}$	UCESS fixed O&M price [GBP/kW/year]
$\rho_{B_OM_v}$	BESS variable O&M price [GBP/kW/h]
$\rho_{UC_OM_v}$	UCESS variable O&M price [GBP/kW/h]
T_{B_hr}	Operation hours of BESS [h]
T_{UC_hr}	Operation hours of UCESS [h]
λ_{dep}	Depreciation coefficient of BESS
k_{SFF}	Definition of sinking fund factor
C_{sub}	Substation energy cost [GBP/day]
$\rho_{grid,t}$	Cost of power from utility grid [GBP/kWh]
C_{dem}	Demand charge [GBP/day]
ρ_{dem}	Price of demand charge [GBP/kW]
P_{max_15min}	Maximum averaged substation power [W]
T	Total system operation time [s]
U_{t_rate}	Train rated voltage [V]
P_{au}	Auxiliary power [W]
R_{line}	Resistance of railway line [Ω]
R_t	Resistance of train [Ω]
R_{sub}	Resistance of substation [Ω]

Abbreviation

URT	Urban railway transit
ESS	Energy storage system
HESS	Hybrid energy storage system
RES	Renewable energy source
PV	Photovoltaic
RBE	Regenerative braking energy
UC	Ultracapacitor
UCESS	Ultracapacitor energy storage system
BESS	Battery energy storage system
CTS	Conventional traction system
SOC	State of charge
BOP	Balance of plant
O&M	Operation and maintenance
SFF	Sinking fund factor
CFPSO	Particle swarm optimization with compression factor

I. INTRODUCTION

Urban railway transit has gained great development in most modern cities, considered as the most economical and environmentally friendly transportation in daily life [1-3]. With the acceleration of decarbonization in the global world, reducing the energy consumption of URT has become a critical problem.

Some methods of reducing energy consumption based on URT system have been widely investigated. One of them is the timetable optimization. It can improve the utilization rate of regenerative braking energy (RBE) by increasing the overlapping time [4, 5]. Another one is the driving profile optimization, and this can directly decrease the train vehicle traction energy demand in URT [6-8]. But these two methods have great limitations on further reducing energy consumption. Energy storage system (ESS) provides a more efficient approach to reduce the energy consumption of traction substation. It can further increase the utilization of regenerative braking energy of URT by storing and transferring it back to URT system. Currently, battery and ultracapacitor are the two popular types of ESS applications in energy system. Most research conducted has been related to improving the energy efficiency of URT by ESS. [9] proposed a dynamic module of battery energy storage system (BESS) considering the SOC and charge/discharge threshold, and the method reduced 590kW substation peak power. [10] designed converter control strategy for ESS and optimized dynamic performance of the ESS. Furtherly, [11] proposed distributed cooperative control strategy for URT with ESS based on a value decomposition network. [12] designed a smart control strategy for ESS and RBE in URT system, reducing the energy consumption of substation. But the economy issue caused by ESS sizing is a key factor in actual operation.

For single-type ESS, its sizing optimization brings a great challenge for energy system operation, and most of research has been conducted by considering economy and environment. [13] investigated a novel method of joint sizing and siting for UCESS in URT, by comparing various siting and sizing solutions between two substations. [14] utilized a bi-objective nonlinear mathematical model to address the optimal siting and sizing of UCESS. An energy saving of 1730 kWh has been achieved in the simulation based on the real data of Italian URT line. [15] proposed a model to determine the optimal installation location of UCESS, and a benefit of 188% the initial investment is gained. For UCESS, it is hard to achieve further energy saving due to its high investment cost and low energy density. In BESS application, researchers like [3] tested the energy-saving capability of BESS with different capacities. [16] utilized the genetic algorithm to optimize the sizing, charge and discharge limits of BESS, and improved energy saving by 30% in URT system. However, BESS needs to avoid charging or discharging frequently due to the battery degradation, which is also a main focus in cooperation with URT [17]. Thus, the single-type ESS usually has certain limitation in operation due to its characteristics of power density or energy density.

The HESS, consisting of BESS and ultracapacitor energy storage system (UCESS), can achieve both high-power density and high-energy density characteristics. It has been widely proven that it can support the power grid operation and

renewable energy sources better than single-type ESS [18]. However, the related cost defined by the HESS rated capacity and power will affect the system operation cost. Besides, HESS requires a more complex and efficient control to achieve the cooperation between UCESS and BESS. Thus, HESS sizing and control strategy or energy management are crucial factors in the design and operation of URT.

Regarding the HESS sizing optimization, it is hard to achieve economy operation and efficient control at the same time because of the high investment cost of UCESS and high operation cost of BESS. The multi-level optimization has become an efficient method to solve the above problem. [19] proposed a bi-level optimization model for the sizing and operation of HESS in railway, considering operation cost and battery degradation. The proposed method helped one substation achieve 8.69% annual saving. Similarly, [20] obtained the optimal sizing of HESS in high-speed railway by minimizing the system operation cost. Optimization model is also considered as a two-level structure, achieving cost saving by 30.95%. [21] aimed at traction power supply system with HESS and renewable energy source (RES), and it proposed a two-layer optimization method. A 13.55% of cost reduction is achieved by sparrow search algorithm. Sizing optimization of URT is usually conducted with energy management, but ignores the system operation states.

Also, many researchers have already investigated the optimization of HESS sizing and energy management in electric vehicles, microgrids, and power grids. Different from URT, only UC cost [22] or HESS cost [23] is considered as objective function with battery lifespan to optimize the HESS sizing in electric vehicles. Similarly, [24] also considered unserved and surplus energy as penalty cost for HESS sizing optimization in microgrid. [25] utilized multi-objective solution to optimize the location and capacity of HESS, reducing line loss and electricity cost in power grid. This kind of HESS sizing optimization (in electric vehicles, microgrids, and power grids) is usually solved by the multi-objective function with load or power profile. The system operation stability which may be affected by control strategy has not been focused on as well.

The control strategies of ESS or HESS, which usually ignore the operation cost, mainly aim to investigate the optimal operation states of the URT. Regarding power of substation, some researchers utilized the ESS to achieve the peak shaving of substation [26]. Similarly, [27] investigated different charging and discharging thresholds of UCESS, achieving the maximum utilization of RBE based on the different train operation states. Similarly, [28] designed a real-time and optimal control for URT and UCESS, which can adjust UCESS control threshold dynamically according to the states of trains. These studies provide an efficient approach regarding the control optimization of URT with ESS, improving the operation stability of substation. As for control strategy in HESS, not only the control strategy but also the cooperation between UCESS and BESS should be focused on. Usually, the UCESS is applied to extend the battery life of BESS, while the BESS will cover the capacity shortage of UCESS. Thus, the battery degradation is a main focus in control optimization of HESS. [29] focused on extending the battery service life in a micro-grid by optimizing the ratio of UC unit's charge and discharge times,

and the problem is solved by an intelligent algorithm. In terms of system operation stability, [30] utilized three-stage scheduling (day-ahead, 15-minute ahead, and real-time) for HESS to track feed-in PV panels, eliminating the uncertainty of renewable energy sources. In summary, the sizing and control strategy of HESS is still a crucial problem in URT system, which has a markable impact on system economy and operation stability (like substation peak power and voltage fluctuations).

Current research usually utilizes the power profile of URT to optimize the sizing and energy management of HESS in URT. Other operation states of the system, like traction substation power and voltage, may be ignored. Thus, this research proposes a bi-level optimization of HESS sizing and control strategy for URT, which considers the substation peak power and voltage range. The master level will optimize the rated capacity and power of HESS by minimizing the system daily operation cost, and then the control strategy of HESS will be optimized at slave level according to different timetables. To be specific, the substation operation stability is enhanced (substation peak power and voltage fluctuations are reduced) by the HESS control strategy and demand charge in slave level of optimization. The main contributions of this research are:

1. Based on the equivalent model of URT with HESS, a bi-level optimization method of HESS sizing and control strategy in URT is designed. The method aims to reduce the total daily cost and improve the URT substation operation stability (including the reduction on substation peak power and voltage range).

2. Based on Merseyrail line with whole-day operation, the proposed method is compared with conventional traction system (CTS) and CTS with single-type ESS, and the impact of different optimization strategies is analyzed.

The rest of this paper is organized as follows. Section II describes the modeling of the system, including train vehicle, substation, railway line, HESS model. Then, the power flow analysis method of the URT with HESS is introduced; in Section III, the proposed bi-level optimization is introduced. The case study based on Merseyrail line in UK is illustrated in Section IV.

II. MODELING OF URT WITH HESS

This research is conducted in the URT with HESS, and its basic structure is shown in Fig. 1. The HESS is installed in substation, which is connected to a DC busbar which is directly linked to the traction substation or third rail. The HESS can discharge to provide the traction power and be charged by regenerative braking energy (RBE). The RBE is generated by braking trains and then injected to the substation.

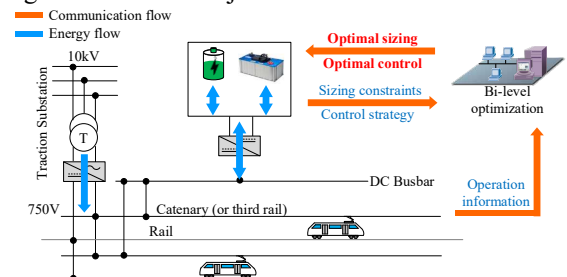


Fig. 1. Topology of the traction system with HESS

A. Urban railway transit model

1) Single train movement model

The single train movement model can be obtained by its mass and velocity, which can be utilized to calculate the train traction power and regenerative braking power. The single train moving along the rail path is described via (1) [31].

$$\begin{cases} m_{eq} \frac{dv}{dt} = F_{veh} - F_t(v, s) \\ m_{eq} = m_0(1 + \lambda) + m_1 \\ \frac{ds}{dt} = v \end{cases} \quad (1)$$

$$F_t(v, s) = k_0(s) + k_1v + k_2v^2 \quad (2)$$

Where m_{eq} is the train mass, v represents the train velocity, F_{veh} is the train traction force or brake force. m_0 , m_1 are empty train mass and load mass, and λ is dimensionless rotating mass factor. k_0 , k_1 , and k_2 are resistance coefficients derived from the actual train shape and its powertrain.

According to different work states of train (accelerating, cruising, coasting, and braking), the power of train will be calculated separately. The train obtains the traction power from the catenary or third rail when it is accelerating or cruising and generates the regenerative braking energy (RBE) when it is braking. Thus, its traction power and regenerative braking energy can be obtained by (3) to (5):

$$P_{me} = F_{veh} v \quad (3)$$

$$P_{el} = \begin{cases} P_{me} / \eta & \text{if } P_{me} \geq 0 \\ P_{me} \eta & \text{if } P_{me} < 0 \end{cases} \quad (4)$$

$$I_t = \frac{P_{el}}{U_1} \quad (5)$$

Where P_{me} represents the train mechanical power, and F_{veh} is traction force. P_{el} is the train electrical power. I_t is the current, and the U_1 is the catenary voltage, η is the efficiency of traction chain conversion.

2) Traction network model

The URT traction network, including traction substations, is modeled by the equivalent circuit model shown in Fig. 2, the similar modeling method can be found in [27]. The substation equivalent model (non-reversible) includes a voltage source and a resistance, and the voltage of substation U_{sub} can be expressed as equation (6). R_{sub} , U_{sub} , and I_{sub} are the substation equivalent resistance, voltage and current. U_{oc} is the substation no-load voltage.

$$U_{sub} = U_{oc} - I_{sub} R_{sub} \quad (6)$$

The DC railway line is modeled as a time-varying resistance R_{line} , which represents the train real-time location caused by its movement. The train is modeled as a power source or a load. V is the nodal voltage, and M is the total number of nodes in the whole system, n and k are the number of substations and trains.

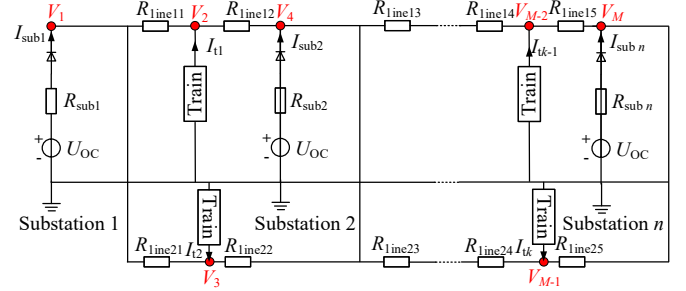


Fig. 2. URT traction network equivalent model

B. HESS model

HESS model includes the battery and ultracapacitor in this research. The model for each part is considered separately.

1) BESS equivalent model

The lead-acid battery is chosen in this research, as it has been widely applied in related research [20, 32]. The battery model usually consists of a bidirectional DC/DC converter and battery cell, which is simulated by an equivalent resistance and a voltage source (shown in Fig. 3), and the detailed equations are shown in equation (7) to (9).

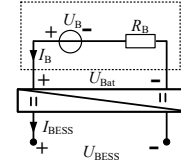


Fig. 3. Battery equivalent model

$$U_{Bat} = U_B - I_B R_B \quad (7)$$

$$U_{BESS} = (U_{Bat} I_B) / I_{BESS} \quad (8)$$

$$SOC_B = SOC_{B_initial} - \frac{\int_0^T I_B(t) dt}{E_{B_rated}} \quad (9)$$

Where R_B , U_{Bat} , I_B are the equivalent resistance, voltage, current of the battery, and U_B is the voltage source of battery. U_{BESS} , I_{BESS} are the equivalent resistance, voltage, current of the battery. SOC_B and $SOC_{B_initial}$ is the current SOC and initial SOC of battery. E_{B_rated} is the rated capacity of battery. Both charge and discharge efficiency of battery are considered as η_B , which has not been presented in the equations. The lifetime of BESS is more easily affected by charge or discharge action than the UCESS [33]. Due to the much longer lifetime of UCESS than BESS, the degradation is only considered in the BESS.

The detailed analysis of battery degradation is not shown here. Based on rain flow method [32, 34-36], the lifetime of BESS T_{B_life} can be expressed by (10).

$$T_{B_life} = 1 / \left(365 \sum_{i=1}^I k_{cycle} \frac{1}{\alpha_1 e^{\alpha_2 DOD_i} + \alpha_3 e^{\alpha_4 DOD_i}} \right) \quad (10)$$

Where α_1 , α_2 , α_3 , and α_4 are the fixed parameter for lead-acid batteries [36] (operation temperature of battery is supposed as 20 °C all the time.). I is the total battery cycles, k_{cycle} equals 1 for a full cycle while 0.5 for a half cycle, DOD is the depth of discharge (which is decided by the change of battery SOC, $DOD = SOC_{B,i+1} - SOC_{B,i}$).

The full cycles and half cycles of charge and discharge are obtained from a series of sequences, solved by the rain flow counting method [36].

2) UCESS equivalent model

The ultracapacitor model is simulated by its equivalent model, which consists of a resistance R and a capacitance C [11], shown in Fig. 4. The voltage and current of UCESS can be calculated by equation (11) to (14).

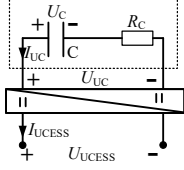


Fig. 4. Ultracapacitor equivalent model

$$U_c(t) = U_c(0) - \frac{1}{C_{UC}} \int_0^t I_{UC}(t) dt \quad (11)$$

$$U_c = U_{UC} + R_c I_{UC} \quad (12)$$

$$U_{UCES} = (U_{UC} I_{UC}) / I_{UCES} \quad (13)$$

$$SOC_{UC_initial} = SOC_{UC_initial} - \frac{\int_0^t I_{UC}(t) dt}{E_{UC_rated}} \quad (14)$$

U_c and I_c are the voltage and current of UC, while the U_{UCES} and I_{UCES} are the voltage and current of UCESS on the catenary side, E_{UC_rated} is the rated capacity of battery. Both charge and discharge efficiency of UC are considered as η_{UC} , which has not been presented in the equations.

3) HESS control strategy

The 24-hour operation of URT with HESS is considered here. Thus, the control strategy has two main parts for different periods, as shown in Fig. 5. First, the HESS will discharge to support the URT system and be charged by RBE from URT, when URT is in service period, similar with [37]. Then, the HESS will only be charged by substation when trains are not operating overnight.

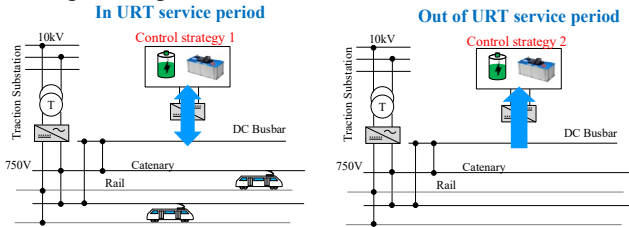


Fig. 5. HESS control strategies in different periods

In URT service period, the HESS will be controlled according to the substation voltage, and then the UCESS and BESS in HESS will cooperate to support the traction system and absorb the RBE. The basic control principle of UCESS and BESS in HESS is shown in Fig. 6. U_{thre_d} and U_{thre_c} are the voltage threshold signal of HESS discharge and charge. P_{UC} and P_B are the power of UCESS and BESS, and the discharge power is the positive value while charge power is the negative value. P_{UC_max} and P_{B_max} are the maximum discharge power of UCESS and BESS (which are equal to the rated power and are positive values), while P_{UC_min} and P_{B_min} are the maximum charge power of UCESS and BESS (which are equal to the minus rated power and are negative value). P_{dis_req} is the

required traction power from URT. P_{ch} is the total RBE injected to the HESS, which is a negative value.

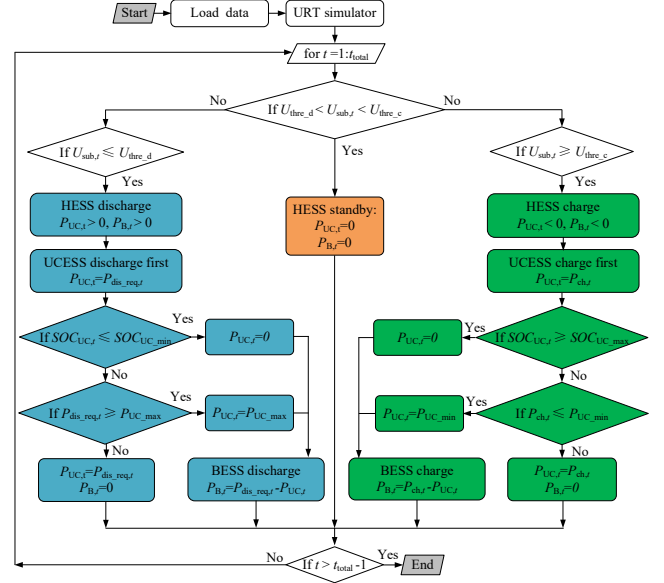


Fig. 6. HESS control principle

In this control strategy, the HESS will discharge when substation voltage is lower than the HESS discharge threshold voltage U_{thre_d} . The UCESS will discharge first to meet the required traction power from control center. If the required power is larger than the maximum power of UCESS or the UCESS SOC reaches the minimal value, the BESS will participate in discharge.

On the contrary, the HESS will be charged when the substation voltage is larger than the HESS charge threshold voltage U_{thre_c} . The UCESS will be charged first by injected RBE. If the RBE power (negative value) is lower than the minimum power of UCESS or the UCESS SOC reaches the maximal value, then the BESS will be charged according to the proposed strategy. Besides, if the substation voltage is from U_{thre_d} to U_{thre_c} , the HESS will be on standby.

When URT is not in service operation time, the HESS will be charged to its initial SOC by constant power from substation, which can ensure the substation operation stability. The charging power P_{HESS_ch} will be defined by equation (15) to (17).

$$P_{HESS_ch} = P_{UC_ch} + P_{B_ch} \quad (15)$$

$$P_{UC_ch} = (SOC_{UC_in} - SOC_{UC_end}) E_{UC_rate} / T_{UC_ch} \quad (16)$$

$$P_{B_ch} = (SOC_{B_in} - SOC_{B_end}) E_{B_rate} / T_{B_ch} \quad (17)$$

Where P_{HESS_ch} , P_{UC_ch} , P_{B_ch} are the charge power of HESS, UCESS, and BESS. SOC_{UC_in} and SOC_{B_in} are the initial SOC of UCESS and BESS. SOC_{UC_end} and SOC_{B_end} are the SOC of UCESS and BESS in the end of trains operation. T_{UC_ch} and T_{B_ch} are total charging time.

If the SOC of UCESS or BESS is larger than the initial value, the UCESS or BESS will not be charged anymore.

C. Power flow analysis of URT with HESS

1) System power flow overview

Conventional power flow analysis of URT only considers the traction substation, railway line, and train vehicle.

2) Power flow analysis

The power flow of URT with ESS is based on nodal voltage equations. In the equivalent model of the URT, the HESS is connected to the traction substation in parallel.

According to the equivalent circuit model of the system shown in Fig. 2, the basic nodal voltage equation of URT system is shown in (18)-(21). To be specific, each value of R_{line} is different and decided by the train real-time position between two nodes. Y is the admittance of R .

$$[V] = [Y]^{-1}[I] \quad (18)$$

Where

$$[V] = [V_1 \ V_2 \ \dots \ V_M]^T \quad (19)$$

$$[I] = [I_{sub1} \ I_{t1} \ \dots \ I_{subn}]^T \quad (20)$$

$$[Y] = \begin{bmatrix} Y_{line11} + Y_{line21} & -Y_{line11} & -Y_{line21} & \dots & 0 \\ -Y_{line11} & Y_{line11} + Y_{line12} & -Y_{line12} & \dots & 0 \\ 0 & -Y_{line21} & Y_{line21} + Y_{line22} & \dots & 0 \\ \dots & \dots & \dots & \dots & \dots \\ 0 & 0 & 0 & \dots & Y_{line15} + Y_{line25} \end{bmatrix} \quad (21)$$

In the equivalent model of URT with HESS, HESS is connected to substation in parallel, which means that the U_{HESS} equals U_{sub} . Based on the above nodal equation, the detailed progress of the power flow analysis method of urban rail transit with HESS is shown Fig. 7.

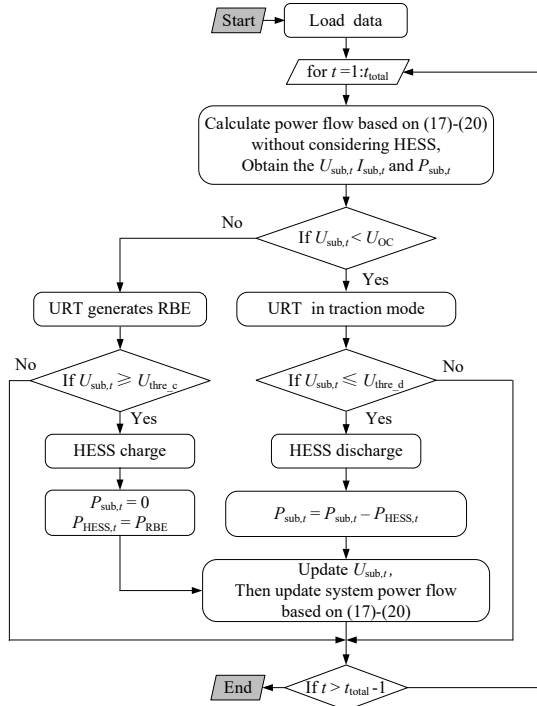


Fig. 7. Process of power flow analysis of URT with HESS

III. OPTIMIZATION OF SIZING AND ENERGY MANAGEMENT OF HESS IN URT

A. Overview

The bi-level optimization is designed here to address the optimization of HESS sizing and operation. The basic structure of the bi-level optimization strategy is shown in Fig. 8. In the first step the system data (URT route data, timetable, electricity price, and HESS parameter) is loaded. Then, URT with HESS simulator will operate based on proposed HESS control strategy.

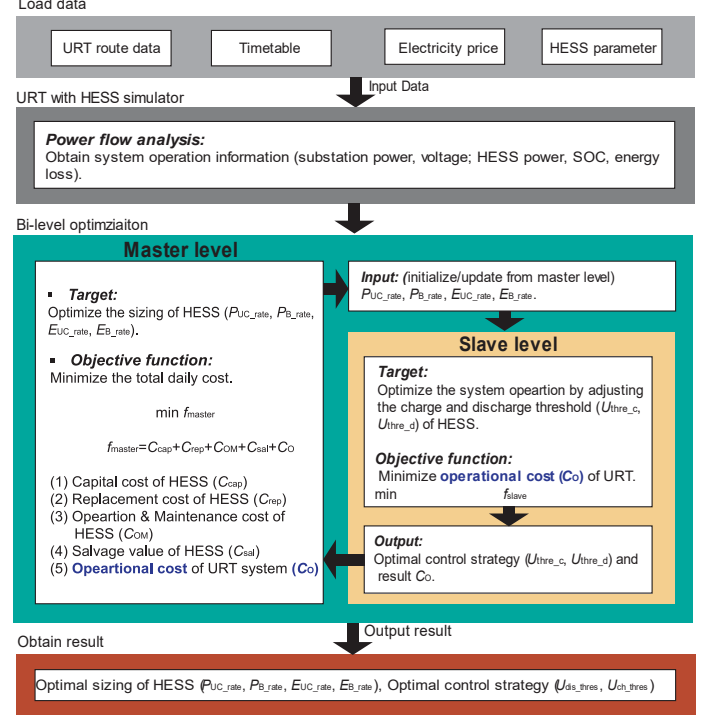


Fig. 8. Bi-level optimization of HESS

The whole optimization strategy consists of master level and slave level. The master level aims to optimize the sizing of HESS in URT, and the rated power and capacity of HESS are the decision variables. Minimizing the total cost of URT with HESS is chosen as the objective function of master level. The total cost of URT with HESS includes capital cost of HESS, cost of HESS battery replacement during the life of the substation (effectively batteries are a consumable), operation and maintenance cost of HESS, salvage value of HESS, and operation cost of URT with HESS [20].

As for slave level, the optimization of energy management is conducted, considering URT operation stability (substation peak power and voltage fluctuations), operational cost of URT, and battery degradation of HESS.

B. Master level

1) Objective function of master level

The master level will optimize the rated power and capacity of HESS by considering the comprehensive cost of HESS. The objective function f_{master} is shown by (22) and (23).

$$\min f_{master} = C_{HESS} + C_{URT} \quad (22)$$

$$C_{HESS} = C_{cap} + C_{rep} + C_{OM} - C_{sal} \quad (23)$$

Where C_{cap} represents the capital cost of HESS, C_{rep} is the replacement cost of battery, C_{OM} is the operation and

maintenance (O&M) cost, and the C_{sal} is the salvage value of battery.

a) Capital cost of HESS

The HESS has four main parts in this research: battery, ultracapacitor, electronic system, and balance of plant equipment (BOP). The BOP devices usually include protective devices, monitoring, and control systems. The capital cost of HESS can be obtained by equation (24) and (25).

$$C_{cap} = \frac{1}{T_{op}} (\rho_{B_p} P_{B_rate} + \rho_{B_E} E_{B_rate} + \rho_{UC_p} P_{UC_rate} + \rho_{UC_E} E_{UC_rate} + \rho_{bop} P_{HESS_rate}) k_{CRF} \quad (24)$$

$$k_{CRF} = \frac{r_0(1+r_0)^{T_{proj}}}{(1+r_0)^{T_{proj}} - 1} \quad (25)$$

Where T_{op} is the operation days of HESS, ρ_{B_p} is the price of the rated battery power, ρ_{UC_p} is the price of the rated ultracapacitor power, ρ_{B_E} is the price of the rated battery capacity, ρ_{UC_E} is the price of the rated battery capacity. ρ_{bop} is the price related to BOP. k_{CRF} is the capital recovery factor, which is the ratio of a constant annuity to the present value of receiving that annuity for a given length of time. T_{proj} is the project service period in years and r_0 is the annual discount rate.

b) Replacement cost HESS

The lifetime of battery is usually less than the whole project period. Thus, the battery should be replaced regularly when its end of life has been reached. The replacement cost of battery during the whole project period will be averaged on each day, and the replacement cost C_{rep} is shown in equation (26) to (28):

$$C_{rep} = \frac{1}{T_{op}} k_{CRF} \sum_{n=1}^{N_{rep}} [\rho_{BE_rep} E_{B_rate} k_{PVF,n}] \quad (26)$$

$$k_{PVF} = (1+r_0)^{-nT_{B_life}} \quad (27)$$

$$N_{rep} = \left\lceil \frac{T_{proj}}{T_B} \right\rceil - 1 \quad (28)$$

N_{rep} represents the total number of replacements of BESS during the calculation period, n is the replacement number of the BESS, ρ_{BE_rep} is replacement cost of the capacity of battery. KPVF is present value factor that is used to derive the present value of a cash receipt in the future.

c) Operation and maintenance cost of HESS

The O&M cost usually includes the fixed O&M annual cost (C_{OM_f}) and variable cost O&M (C_{OM_v}). The variable cost of O&M cost can be obtained by multiplying with yearly operating hours, shown in equation (29) to (31).

$$C_{OM} = C_{OM_f} + C_{OM_v} \quad (29)$$

$$C_{OM_f} = \frac{1}{T_{op}} (\rho_{B_OM_f} P_{B_rate} + \rho_{SC_OM_f} P_{SC_rate}) \quad (30)$$

$$C_{OM_v} = T_{B_hr} \rho_{B_OM_v} P_{B_rate} + T_{SC_hr} \rho_{SC_OM_v} P_{SC_rate} \quad (31)$$

Where $\rho_{B_OM_f}$ and $\rho_{UC_OM_f}$ are the fixed O&M cost of battery and ultracapacitor, $\rho_{B_OM_v}$ and $\rho_{UC_OM_v}$ are the variable O&M cost of battery and ultracapacitor. T_{B_hr} and T_{UC_hr} are the operation hours of battery and ultracapacitor in one day.

d) Salvage value

The salvage value C_{sal} represents the resale value considering the rest life cycle of battery. This value can be estimated by equation (32) and (33).

$$C_{sal} = \lambda_{dep} \frac{(N_{rep} + 1) T_{B_life} - T_{proj}}{T_{op} T_{B_life}} \rho_{Bp_rep} P_{B_rate} k_{SFF} \quad (32)$$

$$k_{SFF} = \frac{r_0}{(1+r_0)^{T_{proj}} - 1} \quad (33)$$

Where λ_{dep} is the depreciation coefficient for the recovery of battery cells. ρ_{Bp_rep} is the price of the batter rated power. k_{SFF} is the definition of sinking fund factor (SFF).

2) Constrains of master level

The master level aims to obtain the optimal sizing of HESS including the rated power and capacity, which could have a minimal operational daily cost of the URT with HESS. Thus, the decision variables will be limited by constraints (34) to (37).

$$P_{B_rate_min} \leq P_{B_rate} \leq P_{B_rate_max} \quad (34)$$

$$E_{B_rate_min} \leq E_{B_rate} \leq E_{B_rate_max} \quad (35)$$

$$P_{UC_rate_min} \leq P_{UC_rate} \leq P_{UC_rate_max} \quad (36)$$

$$E_{UC_rate_min} \leq E_{UC_rate} \leq E_{UC_rate_max} \quad (37)$$

C. Slave level

1) Objective function of slave level

The control strategy of HESS will be optimized here to obtain the minimal operational cost of traction substation.

The objective function of slave level is expressed by (38) and (39).

$$\min f_{salve} = C_o \quad (38)$$

$$C_o = C_{sub} + C_{dem} \quad (39)$$

The grid energy cost C_{sub} of traction substation can be expressed by (40).

$$C_{sub} = \sum_{t=1}^T \rho_{grid,t} P_{sub,t} \quad (40)$$

Where $\rho_{grid,t}$ is the cost of the substation power from the utility grid at time = t , while the $p_{sub,t}$ is the substation power from the utility grid at time = t .

The demand charge is considered here according to the maximum value of the averaged substation active power (usually averaged over a 15-minute period [38]), shown in (41).

$$C_{dem} = \rho_{dem} \bar{P}_{max_15min} \quad (41)$$

Where ρ_{dem} is the price of demand charge, \bar{P}_{max_15min} is averaged substation active power.

The substation energy consumption and averaged substation active power are determined by the substation peak power. The HESS charge and discharge threshold will be optimized to obtain an optimal operational cost.

2) Constraints of slave level

The charge and discharge threshold of HESS (shown in Fig. 6) will be optimized, and these two variables should be subject to following constraints (42) to (43).

$$U_{thre_d_min} \leq U_{thre_d} \leq U_{thre_d_max} \quad (42)$$

$$U_{thre_c_min} \leq U_{thre_c} \leq U_{thre_c_max} \quad (43)$$

During the URT operation service, headways may be various in different periods. The control of HESS needs to be optimized separately to gain the optimal result according to different operation characteristics. The power quality of traction substation is also considered here. Thus, to ensure the substation voltage and power stability, the charge and discharge threshold of HESS will be limited to a certain range. For a total

number of I time periods with different headways, each HESS control signal $U_{\text{thre_ci}}$ and $U_{\text{thre_di}}$ should be subject to following constraints (44) and (45), which means that the substation voltage difference between adjacent time periods is no more than $U_{\text{sub_fluc}}$. $U_{\text{sub_fluc}}$ is set as 1 V in this research.

$$|U_{\text{thre_c1}} - U_{\text{thre_ci}}| \leq U_{\text{sub_fluc}}, \quad i = 1, \dots, I \quad (44)$$

$$|U_{\text{thre_d1}} - U_{\text{thre_di}}| \leq U_{\text{sub_fluc}}, \quad i = 1, \dots, I \quad (45)$$

D. Solving method

According to the nonlinear and multiple-objective characteristics of the proposed bi-level optimization model, the intelligence algorithm will be applied here to solve the problem, which has been proven its validity and efficiency in similar sizing optimization research [18, 39]. The particle swarm optimization with compression factor (CFPSO) is chosen here, due to the CFPSO has a great performance in global exploration [40]. The velocity and position of each particle will be updated by equation (46) to (48) [40].

$$\mathbf{X}_m^k = [X_{m,1}^k, \dots, X_{m,i}^k] \quad (46)$$

$$V_{mi}^k = \alpha[V_{mi}^{k-1} + c_1 r_1 (P_{mi}^{k-1} - X_{mi}^k) + c_2 r_2 (G_{mi}^{k-1} - X_{mi}^k)] \quad (47)$$

$$X_{mi}^k = X_{mi}^{k-1} + V_{mi}^{k-1} \quad (48)$$

Where k is the iteration number, m is the particle number, and i is the variable number. P and G are the positions of optimal result of the particle and particle swarms. α is compression coefficient, c_1 and c_2 are acceleration coefficients, and r_1 and r_2 are random numbers (which are in the range of $[0,1]$), shown in equation (49).

$$\alpha = \frac{2}{|2 - c - \sqrt{c^2 - 4c}|}, \quad c = c_1 + c_2 \quad (49)$$

In each level, the number of search agents is 50 and the maximum number of iterations is set as 50 to ensure that the optimal result can be obtained, $c_1=2$, $c_2=2$.

The detailed optimization process is shown in Fig. 9. In the solving process, decision variables are considered as discrete value within a defined search domain, each with a fixed step size. The search step for P_{UC_rated} and P_{B_rated} are 0.01MW, E_{UC_rated} and E_{B_rated} for are 0.1 kWh, for $U_{\text{thre_c}}$ and $U_{\text{thre_d}}$ are 0.1 V.

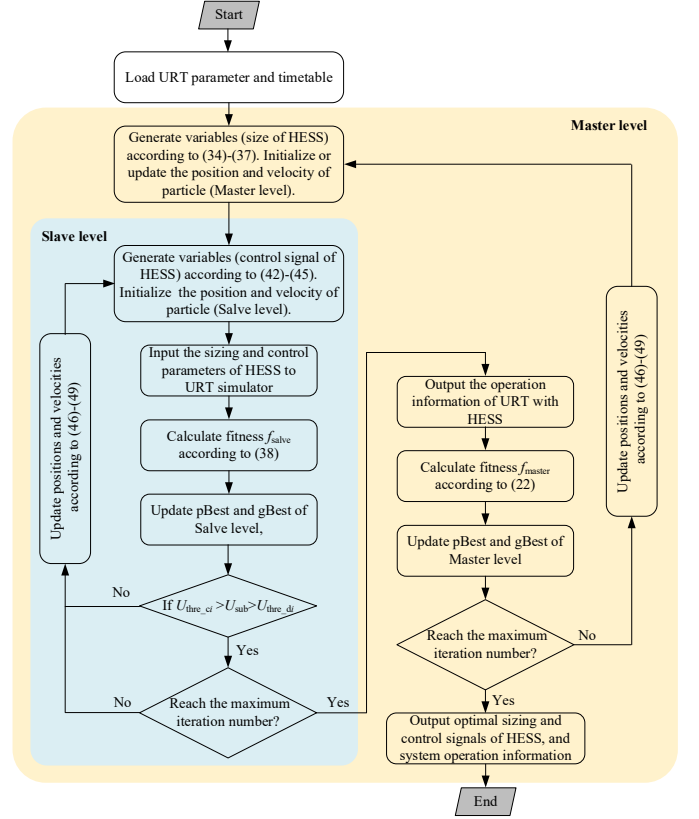


Fig. 9. Solving process of proposed bi-level optimization

IV. SIMULATION AND ANALYSIS

A. Parameter setting

The case study is conducted based on the Merseyrail line shown in Fig. 10. The selected line is between Hamilton Square and West Kirby, which is a 14.06 km straight line with 11 stations. The total journey time is around 26 min.

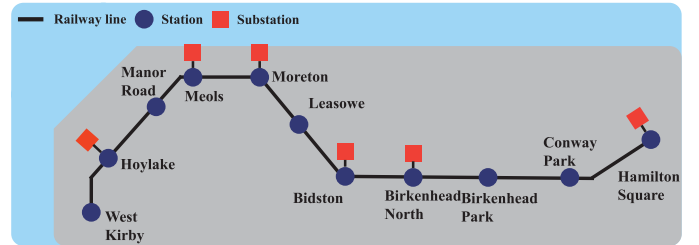


Fig. 10. Merseyrail line

The detailed data of the selected Merseyrail line is shown in Table I and Table II. Due to space limitation, the HESS is installed in substation Moreton (substation 3) in this research. The sizing and control strategy of the HESS in substation Moreton will be optimized by the proposed method. The simulation result will focus on the substation Moreton, while the simulation process is based on the whole line shown in Fig. 10 within 24-hour operation.

The train operation time is from 05:51 to 23:01, and the detailed timetable is shown in TABLE I. The whole train operation period is divided into four periods according to different headways (T1, T2, T3, and T4). The substation location is shown in TABLE II, while parameters of the

Meyseryrail line and train are shown in TABLE III. Besides, the electricity price considers the time of use, which is shown in TABLE IV.

TABLE I . TIMETABLE OF MERSEYRAIL LINE

Period	headway
05:51 to 06:51 (T1)	30 min
06:51 to 18:36 (T2)	15 min
18:36 to 19:01 (T3)	25 min
19:01 to 23:01 (T4)	30 min

TABLE II . LOCATION OF SUBSTATION

No.	Station	Location (km)	No.	Station	Location (km)
1	West Kirby	0	7	Biston	9.1
2	Hoylake	2.02	8	Birkenhead North	10.7
3	Manor Road	2.74	9	Birkenhead Park	12.11
4	Meols	3.95	10	Conway Park	13.34
5	Moreton	6.8	11	Hamilton Square	14.06
6	Leasowe	7.69			

TABLE III . PARAMETERS OF THE RAILWAY SYSTEM

U_{oc}	800 V	R_{sub}	0.0161 Ω
R_{line}	0.02 Ω/km	P_{au}	75 kW
R_t	0.015 Ω	Train mass	101 t
U_{b_rate}	825 V	U_{t_rate}	750 V

TABLE IV . TIME OF USE ELECTRICITY PRICE

Period	Price (GBP/kWh)	Period	Price (GBP/kWh)
0:00-6:00	0.05	11:00-18:00	0.1
6:00-8:00	0.1	18:00-21:00	0.16
8:00-11:00	0.16	21:00-0:00	0.05

The fixed parameter of HESS including the range of HESS rated power and capacity is given in TABLE V. Besides, the cost of BESS and UCESS is shown in TABLE VI (data refers to [20])

TABLE V . PARAMETERS OF THE HESS

$SOC_{UC,in}$	0.9	η_B	0.8
$SOC_{B,in}$	0.8	η_{UC}	0.95
$SOC_{B,max}$	0.8	Range of $E_{UC\ rated}$	[5, 15]
$SOC_{B,min}$	0.2	Range of $P_{UC\ rated}$	[0.5, 1]
$SOC_{UC,max}$	0.9	Range of $E_B\ rated$	[25, 50]
$SOC_{UC,min}$	0.1	Range of $P_B\ rated$	[0.1, 0.2]

TABLE VI . COST OF THE HESS

Price	Value	Price	Value
$\rho_B E$	515.6	$\rho_B OM f$	2.8
$\rho_{UC E}$	22000.0	$\rho_{UC OM f}$	0
$\rho_B p$	315.3	$\rho_B OM v$	0.3
$\rho_{UC p}$	227.8	$\rho_{UC OM v}$	0
$\rho_{BE rep}$	143.6	λ_{dep}	0.7
ρ_{bop}	74.9	r_0	5%

B. Simulation result

Based on Merseyrail line, four scenarios are set here to verify the proposed method. All scenarios consider the time of use electricity price. The sizing range of UCESS and BESS is shown in TABLE V, considering the limitation of the installation area. To keep the substation operation stable, the substation voltage should be kept within a certain range. In this

research, this range is set as [790V, 810V]. Thus, the search range of HESS charge threshold will be subjected to $800V \leq U_{thre_c} \leq 810V$ and discharge threshold $790V \leq U_{thre_d} \leq 800V$.

TABLE VII . SCENARIO SETTING

Scenario	ESS type	Sizing	Control strategy
S1	None	None	None
S2	UCESS	Optimized	Different parameters for T1 to T4
S3	HESS	Optimized	Same parameter for T1 to T4
S4	HESS	Optimized	Different parameters for T1 to T4

TABLE VII shows the scenario setting of the case study. The single BESS is not considered here due to its power limit, which cannot shave the substation peak power efficiently. In scenario S1, the conventional URT is simulated based on Merseyrail line, and all RBE which could be injected to the substation is wasted in resistance. In Scenario S2, only the UCESS will be installed. Its sizing is optimized by proposed method and control parameters will be optimized separately for different periods. In Scenario S3, HESS will be installed. Its sizing is optimized by proposed method and control parameters will be optimized as same value for all periods. As for Scenario S4, the HESS will be installed. Its sizing is optimized by proposed method and control parameters will be optimized separately for different periods. The optimal results of S2 to S4 are shown in TABLE VIII.

TABLE VIII . OPTIMAL RESULT OF HESS SIZING AND CONTROL SIGNAL

Scenario	S2	S3	S4
$P_{UC\ rated}$ (MW)	0.73	0.70	0.72
$E_{UC\ rated}$ (kWh)	13.60	13	14.30
$P_B\ rated$ (MW)	\	0.15	0.17
$E_B\ rated$ (kWh)	\	40.4	43.40
$U_{thre\ c1}$ (V)	802.5	802.5	802.0
$U_{thre\ c2}$ (V)	802.0	\	801.5
$U_{thre\ c3}$ (V)	802.5	\	802.0
$U_{thre\ c4}$ (V)	802.0	\	801.5
$U_{thre\ d1}$ (V)	793.4	796.5	797.5
$U_{thre\ d2}$ (V)	793.7	\	797.3
$U_{thre\ d3}$ (V)	793.4	\	797.5
$U_{thre\ d4}$ (V)	793.8	\	797.4

The power and location of a single train in up line and down line are shown in Fig. 11, and the red curve represents the train power while the blue one is for train location.

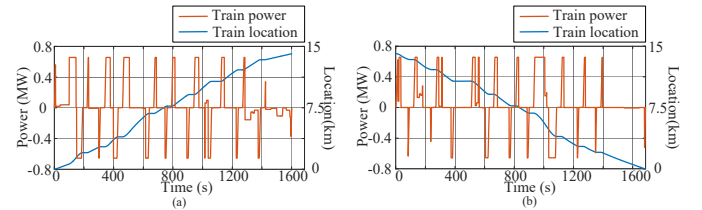


Fig. 11. Power and location of a single train: (a) up line (b) down line

1) Substation Moreton operation analysis

The conventional traction system is simulated according to above setting (S1), which is considered as the benchmark to make comparisons. The all-day operation state of substation Moreton is shown in Fig. 12. The peak power of substation is up to 0.96 MW while the substation voltage fluctuates between 776.0 V and 998.9 V.

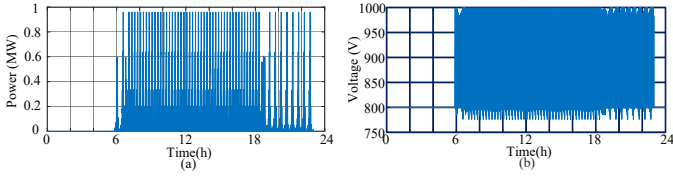


Fig. 12. S1: Power and voltage of substation Moreton

The substation power is reduced remarkably in S2 to S4, shown in Fig. 13. In S2, the substation peak power is 0.25 MW during T1 and T3, and it rises to 0.26 MW during T2 and T4. As for S3, the HESS utilizes the same charging and discharging threshold for each period. So, the substation peak power remains 0.14 MW during the 24-hour operation. The substation has the lowest peak power in S4 (reduced to 0.1MW during T1 and T3, 0.104 MW during T2 and T4).

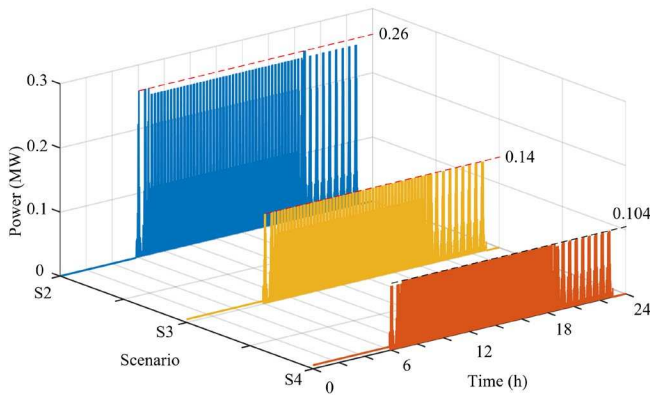


Fig. 13. Comparison of substation power among S2, S3, and S4

The substation voltage in S2 to S4 is shown in Fig. 14. Similar to the substation power, the substation voltage has the lowest fluctuation range in S4, from 802.0 V to 797.5V in T1 and T3, and from 801.5 V to 797.4 V in T2 and T4.

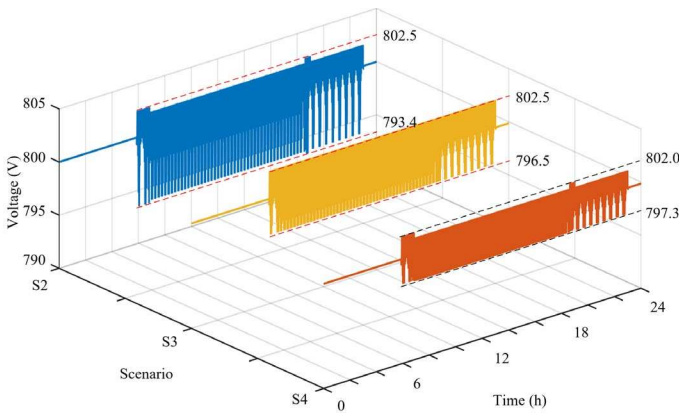


Fig. 14. Comparison of substation voltage among S2, S3, and S4

2) HESS operation analysis of substation Moreton

The 24-hour operation state of UCESS in S2 is shown below (in Fig. 15). The maximum discharge power of UCESS reaches

0.73MW, and the SOC remains at maximum value when trains stop operation.

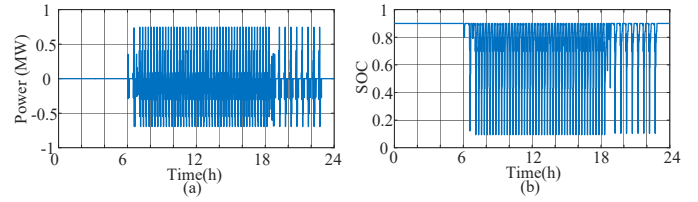


Fig. 15. UCESS operation state in S2

The Fig. 16 and Fig. 17 illustrate the HESS detailed operation states in S3 and S4. The UCESS and BESS discharge power is approximately equal to the rated power in both scenarios. After the train operation period, the UCESS and BESS are charged to the initial SOC value by the substation with constant power.

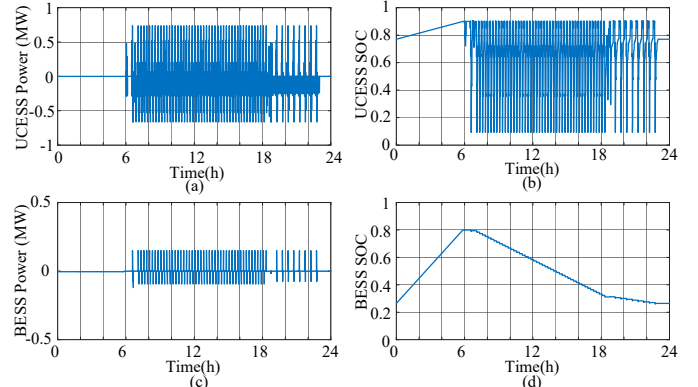


Fig. 16. HESS operation state in S3

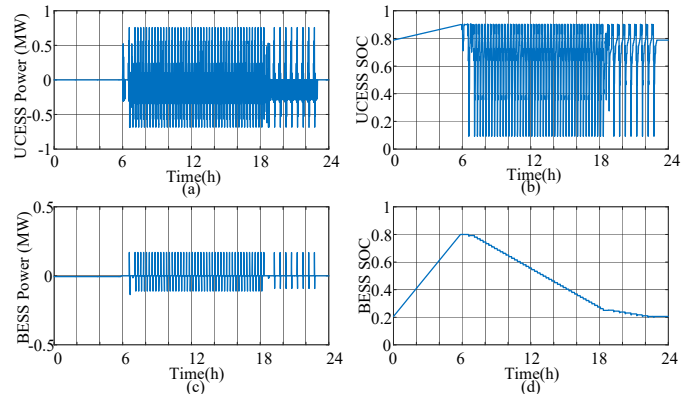


Fig. 17. HESS operation state in S4

The power of UCESS in S4 (0.57MW) is higher than the one in S3 during T3, which leads to a further reduction on substation peak power (0.1 MW) in S4 shown in Fig. 18. A similar result can be seen in T1 period between S3 and S4.

Namly, the HESS discharge and charge thresholds are the same in different operation periods in S3, so the substation voltage shows the most stable state (from 769.5 V to 802.5 V shown in Fig. 14) during train operation. Differently, the HESS thresholds are optimized separately for each period in S4. The maximum and minimum substation voltage show a little difference in different periods, but the difference among each period is lower than 1 V, which is still remarkably stabler than S1.

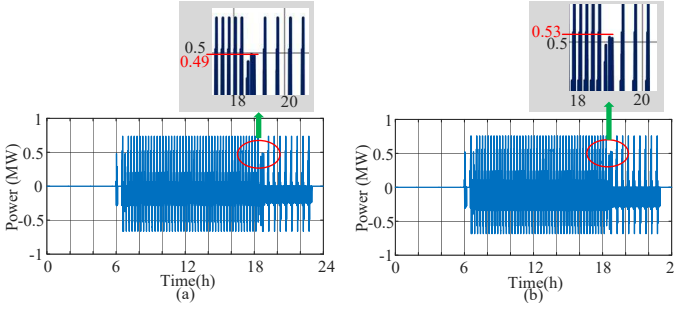


Fig. 18. Comparison of UCESS in S3 and S4: (a) S3 (b) S4

3) Energy and operation cost analysis of substation Moreton

In this section, the S1 (conventional URT) will be utilized as the benchmark value to conduct the comparison among the four scenarios. In S1, there are 1407.6 kWh of RBE can be absorbed by substation Moreton in total potentially.

The energy comparison of each scenario is shown in TABLE IX. The total grid energy consumption of conventional system is 1551.70 kWh (S1). The URT with UCESS in S2 reduces the energy consumption from the grid by 36.23%, while S3 reduces by 50.96%, and 57.35% of grid energy consumption has been decreased in S4. The peak power of substation Moreton is reduced significantly after HESS is installed, especially in S4 (reduced by 89.71%). Besides, the average power of substation (during the train-operation period) can be decreased significantly by HESS with proposed optimization method. Especially in S4, the average power can be decreased by 57.36% compared to S1.

TABLE IX ENERGY COMPARISON OF EACH SCENARIO

Parameter	S1	S2	S3	S4
Energy from grid (kWh)	1551.70	989.58	760.97	661.7
Grid energy saving rate	\	36.23%	50.96%	57.35%
Total RBE (kWh)	1407.60	\	\	\
RBE used (kWh)	\	587.01	873.03	975.35
RBE utilization rate	\	39.92%	62.02%	69.29%
HESS energy loss (kWh)	\	24.89	82.30	85.35
Substation peak power (MW)	0.96	0.26	0.14	0.104
Peak power reduction rate	\	72.92%	85.42%	89.17%
Substation average power (kW)	90.39	57.64	44.33	38.54

The traction power supply of each scenario is shown in Fig. 19. The total energy consumption is increased in S2 to S4 (compared with S1) because of the energy loss in ESS or HESS. However, the energy consumption from the grid is reduced (shown in blue), and S4 decreases most (up to 57.35%). The RBE is utilized most in S4, which accounts for 69.29% of total RBE.

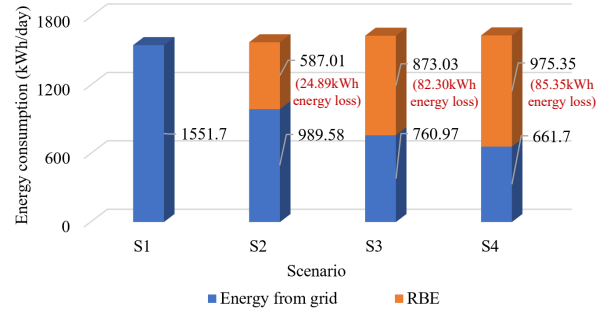


Fig. 19. Traction power supply in different scenarios

The operational cost comparison of each scenario is shown in TABLE X. The conventional URT system will cost 200.5 GBP per day only on grid energy cost and demand charge. The daily cost is reduced to 185.26 GBP when UCESS is installed in S2. HESS can help system further decrease the daily cost (in S3 and S4), although the capital cost of HESS (S4) is much higher than the UCESS in S2.

TABLE X DAILY COST COMPARISON OF EACH SCENARIO

Parameter	S1	S2	S3	S4
Grid energy cost (GBP)	183.90	115.23	89.93	78.60
Grid energy cost saving rate	\	37.34%	51.10%	57.26%
Demand charge (GBP)	16.60	11.09	8.43	7.23
Capital cost (GBP)	\	58.94	79.07	85.10
Replacement cost (GBP)	\	\	2.35	2.52
O&M cost (GBP)	\	\	1.45	1.64
Salvage value (GBP)	\	\	0.02	0.02
Total cost (GBP)	200.50	185.26	181.21	175.08
Total cost saving rate	\	7.60%	9.62%	12.68%
Battery life (year)	\	\	3.89	3.81

The main operational cost of each scenario is shown in Fig. 20, except for the salvage value. URT cost (including grid energy cost and demand charge) is the most in the CTS (up to 200.5 GBP), while the HESS helps to reduce daily cost by at least 7.60%. Especially in S4, the HESS with proposed sizing and control optimization decreases the most on grid energy cost (up to 57.26%) and daily cost (up to 12.68%), although its capital cost could spend 85.10 GBP per day.

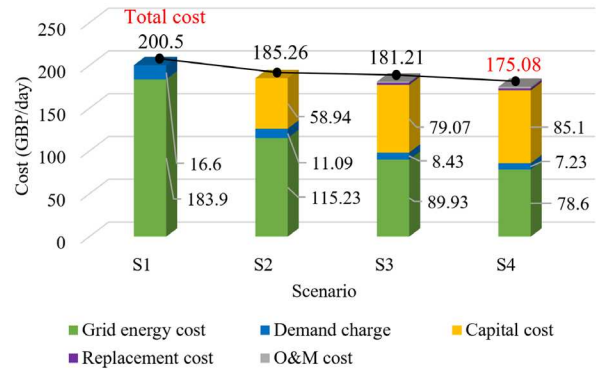


Fig. 20. Daily operational cost in different scenarios

In summary, the proposed method can efficiently help substation to reduce the daily operation cost and improve the operation stability (substation peak power and voltage fluctuations are decreased), according to the result of S3 and S4.

To be specific, the same optimal HESS control parameters (in S3) allow substation to have the most stable states, with a little increase on daily cost compared with S4. The least daily operation cost is achieved in S4, while the substation operation stability is still stable. From a one-year perspective, the grid energy cost of substation Moreton can be saved by 769k GBP during the whole project.

V. CONCLUSION

This research proposes a bi-level optimization method for HESS sizing and control strategy in URT system. The rated power and capacity of UCESS and BESS of HESS are optimized in master level by minimizing the system operation cost. Meanwhile, the control strategy of HESS is optimized in slave level by minimizing the substation operation cost. Based on Merseyrail line, the validity of proposed method has been verified. The reduction in grid energy cost by 57.26% and substation peak power by 89.17% are achieved.

The result also illustrates that:

1. The peak power of substation has been reduced remarkably, which allows that substation transformer capacity can be reduced, the train vehicle with higher traction demand can be applied in the current rail line, and departure intervals can be reduced.
2. The energy consumption of substation can be decreased by more than 50%. As a result, in areas with high energy price, the proposed method can achieve a further cost saving on daily operation.
3. The same optimal control parameter of HESS will bring more stability for substation operation while the operation cost will increase a little, compared with applying different optimal control parameters of HESS for each period with different departure intervals.

However, the siting optimization of HESS in URT is not considered here, and the RBE of the system has not been fully utilized in the proposed method. Future work will investigate the siting and sizing optimization of HESS in URT with renewable energy sources. Meanwhile, the improvement of RBE utilization rate will be focused on.

VI. REFERENCES

- [1] S. Wandelt, Z. Wang, and X. Sun, "Worldwide Railway Skeleton Network: Extraction Methodology and Preliminary Analysis," *IEEE Transactions on Intelligent Transportation Systems*, vol. 18, no. 8, pp. 2206-2216, 2017.
- [2] F. Meng, G. Liu, Z. Yang, M. Casazza, S. Cui, and S. Ulgiati, "Energy efficiency of urban transportation system in Xiamen, China. An integrated approach," *Applied energy*, vol. 186, pp. 234-248, 2017.
- [3] D. I. Fletcher, R. F. Harrison, and S. Nallaperuma, "TransEnergy – a tool for energy storage optimization, peak power and energy consumption reduction in DC electric railway systems," *Journal of Energy Storage*, vol. 30, p. 101425, 2020.
- [4] I. Amit and D. Goldfarb, "The timetable problem for railways," *New York, NY, USA: Gordon and Breach*, pp. 379-387, 1971.
- [5] Y. Bai, Y. Cao, Z. Yu, T. K. Ho, C. Roberts, and B. Mao, "Cooperative Control of Metro Trains to Minimize Net Energy Consumption," *IEEE Transactions on Intelligent Transportation Systems*, vol. 21, no. 5, pp. 2063-2077, 2020.
- [6] R. R. Liu and I. M. Golovitcher, "Energy-efficient operation of rail vehicles," *Transportation Research Part A*, vol. 37, no. 10, pp. 917-932, 2003.
- [7] Z. Tian, N. Zhao, S. Hillmanssen, C. Roberts, T. Dowens, and C. Kerr, "SmartDrive: Traction Energy Optimization and Applications in Rail Systems," *IEEE Transactions on Intelligent Transportation Systems*, vol. 20, no. 7, pp. 2764-2773, 2019.
- [8] B. Ke, C. Lin, and C. Yang, "Optimisation of train energy-efficient operation for mass rapid transit systems," *IET Intelligent Transport Systems*, vol. 6, no. 1, pp. 58-66, 2012.
- [9] Q. Qin, T. Guo, F. Lin, and Z. Yang, "Energy Transfer Strategy for Urban Rail Transit Battery Energy Storage System to Reduce Peak Power of Traction Substation," *IEEE Transactions on Vehicular Technology*, vol. 68, no. 12, pp. 11714-11724, 2019.
- [10] F. Zhu, Z. Yang, H. Xia, and F. Lin, "Hierarchical Control and Full-Range Dynamic Performance Optimization of the Supercapacitor Energy Storage System in Urban Railway," *IEEE Transactions on Industrial Electronics*, vol. 65, no. 8, pp. 6646-6656, 2018.
- [11] F. Zhu, Z. Yang, F. Lin, and Y. Xin, "Decentralized Cooperative Control of Multiple Energy Storage Systems in Urban Railway Based on Multiagent Deep Reinforcement Learning," *IEEE Transactions on Power Electronics*, vol. 35, no. 9, pp. 9368-9379, 2020.
- [12] S. Boudoudouh and M. Maâroufi, "Smart control in a DC railway by Multi Agent System (MAS)," in *2016 International Conference on Electrical Systems for Aircraft, Railway, Ship Propulsion and Road Vehicles & International Transportation Electrification Conference (ESARS-ITEC)*, 2-4 Nov. 2016 2016, pp. 1-6.
- [13] V. Calderaro, V. Galdi, G. Graber, and A. Piccolo, "Siting and sizing of stationary SuperCapacitors in a Metro Network," in *AEIT Annual Conference 2013*, 3-5 Oct. 2013 2013, pp. 1-5.
- [14] R. Lamedica, A. Ruvio, E. Tanzi, and L. Palagi, "O.Si.Si: Optimal Sizing and Siting of stationary storage systems in railway electrical lines using a blackbox integer model," *Journal of Energy Storage*, vol. 51, p. 12, 2022.
- [15] D. Roch-Dupré, T. Gonsalves, A. P. Cucala, R. R. Pecharrómán, Á. J. López-López, and A. Fernández-Cardador, "Determining the optimum installation of energy storage systems in railway electrical infrastructures by means of swarm and evolutionary optimization algorithms," *International Journal of Electrical Power & Energy Systems*, vol. 124, p. 106295, 2021.
- [16] S. Nallaperuma, D. Fletcher, and R. Harrison, "Optimal control and energy storage for DC electric train systems using evolutionary algorithms," *Railway Engineering Science*, vol. 29, no. 4, pp. 327-335, 2021.
- [17] S. d. I. Torre, A. J. Sánchez-Racero, J. A. Aguado, M. Reyes, and O. Martínez, "Optimal Sizing of Energy Storage for Regenerative Braking in Electric Railway Systems," *IEEE Transactions on Power Systems*, vol. 30, no. 3, pp. 1492-1500, 2015.
- [18] F. Zhang, Z. Hu, K. Meng, L. Ding, and Z. Dong, "HESS Sizing Methodology for an Existing Thermal Generator for the Promotion of AGC Response Ability," *IEEE Transactions on Sustainable Energy*, vol. 11, no. 2, pp. 608-617, 2020.
- [19] S. Gao, Q. Li, X. Huang, Q. Ma, W. Liu, and S. Tang, "Optimal sizing and operation of hybrid energy storage systems in co-phase traction power supply system considering battery degradation," *IET Generation, Transmission & Distribution*, vol. 17, no. 9, pp. 2038-2054, 2023.
- [20] Y. Liu, M. Chen, S. Lu, Y. Chen, and Q. Li, "Optimized sizing and scheduling of hybrid energy storage systems for high-speed railway traction substations," *Energies*, vol. 11, no. 9, p. 2199, 2018.
- [21] M. Chen, Z. Liang, Z. Cheng, J. Zhao, and Z. Tian, "Optimal Scheduling of FTPSS With PV and HESS Considering the Online Degradation of Battery Capacity," *IEEE Transactions on Transportation Electrification*, vol. 8, no. 1, pp. 936-947, 2022.
- [22] L. Wang, M. Li, Y. Wang, and Z. Chen, "Energy Management Strategy and Optimal Sizing for Hybrid Energy Storage Systems Using an Evolutionary Algorithm," *IEEE Transactions on Intelligent Transportation Systems*, vol. 23, no. 9, pp. 14283-14293, 2022.
- [23] M. Li, L. Wang, Y. Wang, and Z. Chen, "Sizing Optimization and Energy Management Strategy for Hybrid Energy Storage System Using Multiobjective Optimization and Random Forests," *IEEE Transactions on Power Electronics*, vol. 36, no. 10, pp. 11421-11430, 2021.
- [24] P. N. D. Premadasa and D. P. Chandima, "An innovative approach of optimizing size and cost of hybrid energy storage system with state of charge regulation for stand-alone direct current microgrids," *Journal of Energy Storage*, vol. 32, p. 101703, 2020.
- [25] N. Yan, B. Zhang, W. Li, and S. Ma, "Hybrid energy storage capacity allocation method for active distribution network considering demand side response," *IEEE Transactions on Applied Superconductivity*, vol. 29, no. 2, pp. 1-4, 2018.

- [26] H. Dong, Z. Tian, J. W. Spencer, D. Fletcher, and S. Hajiabady, "Coordinated Control Strategy of Railway Multisource Traction System With Energy Storage and Renewable Energy," *IEEE Transactions on Intelligent Transportation Systems*, vol. 24, no. 12, pp. 15702-15713, 2023.
- [27] Z. Yang, Z. Yang, H. Xia, and F. Lin, "Brake Voltage Following Control of Supercapacitor-Based Energy Storage Systems in Metro Considering Train Operation State," *IEEE Transactions on Industrial Electronics*, vol. 65, no. 8, pp. 6751-6761, 2018.
- [28] Z. Yang, F. Zhu, and F. Lin, "Deep-Reinforcement-Learning-Based Energy Management Strategy for Supercapacitor Energy Storage Systems in Urban Rail Transit," *IEEE Transactions on Intelligent Transportation Systems*, vol. 22, no. 2, pp. 1150-1160, 2021.
- [29] Y. Jing, H. Wang, Y. Hu, and C. Li, "A Grid-Connected Microgrid Model and Optimal Scheduling Strategy Based on Hybrid Energy Storage System and Demand-Side Response," *Energies*, vol. 15, no. 3, p. 1060, 2022.
- [30] Z. Liang, Z. Song, J. Wang, X. Wang, and G. Zhang, "Three-stage scheduling scheme for hybrid energy storage systems to track scheduled feed-in PV power," *Solar Energy*, vol. 188, pp. 1054-1067, 2019.
- [31] M. Blanco-Castillo, A. Fernández-Rodríguez, A. Fernández-Cardador, and A. P. Cucala, "Eco-Driving in Railway Lines Considering the Uncertainty Associated with Climatological Conditions," *Sustainability (Switzerland)*, vol. 14, no. 14, 2022.
- [32] N. Anglani, G. Oriti, and M. Colombini, "Optimized Energy Management System to Reduce Fuel Consumption in Remote Military Microgrids," *IEEE Transactions on Industry Applications*, vol. 53, no. 6, pp. 5777-5785, 2017.
- [33] M. A. Tankari, M. B. Camara, B. Dakyo, and G. Lefebvre, "Use of Ultracapacitors and Batteries for Efficient Energy Management in Wind-Diesel Hybrid System," *IEEE Transactions on Sustainable Energy*, vol. 4, no. 2, pp. 414-424, 2013.
- [34] S. Li, P. Zhao, C. Gu, J. Li, S. Cheng, and M. Xu, "Online Battery Protective Energy Management for Energy-Transportation Nexus," *IEEE Transactions on Industrial Informatics*, vol. 18, no. 11, pp. 8203-8212, 2022.
- [35] T. M. Layadi, G. Champenois, M. Mostefai, and D. Abbes, "Lifetime estimation tool of lead-acid batteries for hybrid power sources design," *Simulation Modelling Practice and Theory*, vol. 54, pp. 36-48, 2015.
- [36] C. Amzallag, J. Gerey, J. L. Robert, and J. Bahuaud, "Standardization of the rainflow counting method for fatigue analysis," *International journal of fatigue*, vol. 16, no. 4, pp. 287-293, 1994.
- [37] Y. Liu, Z. Yang, X. Wu, D. Sha, F. Lin, and X. Fang, "An Adaptive Energy Management Strategy of Stationary Hybrid Energy Storage System," *IEEE Transactions on Transportation Electrification*, vol. 8, no. 2, pp. 2261-2272, 2022.
- [38] D. Roch-Dupré, Á. J. López-López, R. R. Pecharrmán, A. P. Cucala, and A. Fernández-Cardador, "Analysis of the demand charge in DC railway systems and reduction of its economic impact with Energy Storage Systems," *International Journal of Electrical Power & Energy Systems*, vol. 93, pp. 459-467, 2017.
- [39] B. Celik, A. Verdicchio, and T. Letrouvé, "Sizing of renewable energy and storage resources in railway substations according to load shaving level," in *2020 IEEE Vehicle Power and Propulsion Conference (VPPC)*, 18 Nov.-16 Dec. 2020 2020, pp. 1-5.
- [40] Z. Yang *et al.*, "Optimal Configuration for Mobile Robotic Grinding of Large Complex Components Based on Redundant Parameters," *IEEE Transactions on Industrial Electronics*, pp. 1-10, 2023.



Zhongbei Tian (Member, IEEE) received the B.Eng in Huazhong University of Science and Technology, Wuhan, China, in 2013. He received the B.Eng. and PhD degree in Electrical and Electronic Engineering from the University of Birmingham, Birmingham, U.K., in 2013 and 2017. He is currently a Lecturer in Electrical Energy Systems at the University of Liverpool. His research interests include railway traction power system modelling and analysis, energy-efficient train control, energy system optimization, and sustainable transport energy systems integration and management.



Joseph W. Spencer received the B.Eng. and Ph.D. degrees in electrical engineering from the University of Liverpool, Liverpool, U.K., in 1981 and 1984, respectively. He is a Professor of Electrical Engineering, the Director of the Centre for Intelligent and Monitoring Systems, and was the Head of the School of Electrical Engineering, Electronics and Computer Science with the University of Liverpool. His current research interests include electrical power equipment and intelligent monitoring systems. Prof. Spencer is a Committee Member of the British Standards Institution and a Fellow of the Institution of Electrical Engineering, U.K.



David Fletcher is Professor of Railway Engineering in the Department of Mechanical Engineering at the University of Sheffield in the United Kingdom. He received his PhD from Sheffield in 1999, and his undergraduate Mechanical Engineering degree from the University of Leeds. Over the past ten years he has been active in research on energy demand reduction and most recently application of energy storage for electrified railway networks. He is active in rail electrification research on the pantograph to overhead line interface, and has focused on a network modelling approach to build on his experience in modelling mechanical aspects of train to infrastructure interaction.



Siavash Hajiabady received the B.Eng in Electrical and Energy Engineering from the University of Birmingham, U.K., in 2011. and Master of Research in Railways Systems engineering and Integration from the University of Birmingham, U.K., in 2013 and also, and PhD degree on condition monitoring of the power converter and gearbox of wind turbines from the University of Birmingham, U.K., in 2018. He is currently a Principal Traction Engineer at ETAP Automation Ltd UK. His research interests include railway traction power system modelling and analysis and green energy supply for the Railway.



Hongzhi Dong (Student Member, IEEE) received the B.S. and M.S. degrees in School of electrical engineering, Southwest Jiaotong University in 2016 and 2019. He is currently a PhD student in the Department of Electrical Engineering and Electronics at the University of Liverpool. His research interests include analysis and control of power system, modelling and optimization of railway system with renewable energy.